MODELLING THE AEOLIAN EROSION THRESHOLDS ON MARS E. Hébrard[1,2], P. Coll[1], F. Montmessin[2], B. Marticorena[1], G. Bergametti[1]. [1]LISA, Universités Paris 12 et Paris 7, CNRS, 61 av. du Général de Gaulle, 94010 Créteil, FRANCE, [2]SA, réduit de Verrières, BP3, route des Gatines, 91371 Verrières-le-Buisson Cedex, FRANCE.
E-mail : hebrard@lisa.univ-paris12.fr.

Introduction: Dust storms have been reported in all seasons on Mars from groundbased and spacecraft observations, across much of the planet and ranging from small local storms covering a few tens of km^2 to planet encircling [1]. Mars Global Circulation Model (MGCM) simulations indicate that the large quantities of dust lifted into the atmosphere during these storms can have a strong impact on the atmospheric thermal structure, the global circulation patterns and thus the climate in general. Further understanding of the origin of these local and global dust storms strongly implies the description of the processes involved in dust rising and transportation from the Martian surface. There have not been enough data available to implement a variable wind stress threshold map for Mars in modern MGCM [2]. However, looking at observations, it is almost certain that aeolian erosion threshold varies from one region to another depending on the ease of dust lifting from the surface, which in turn depends on surface roughness, local circulations, interparticle cohesion and other such factors.

Physical modelling of wind erosion threshold: A recent physical model, applicable on large scales, has been developed at LISA to account for the influence of the surface characteristics on the spatial and temporal variability of dust emission in arid terrestrial environments, by including explicit parameterizations of the aeolian erosion threshold as a function of the surface roughness [3, 4] (Fig. 1). This model has been adapted to Martian conditions.

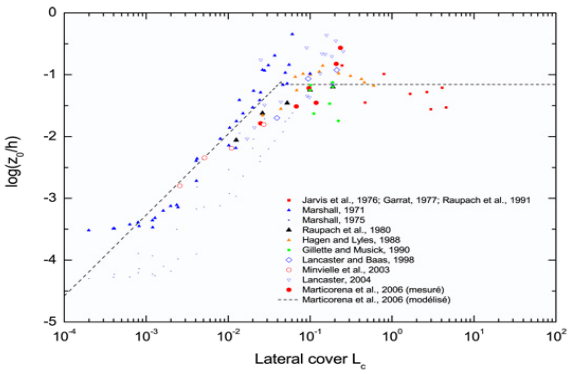

Fig. 1. Logarithm of the ratio of the aerodynamic roughness height Z_0 to the mean roughness elements height h as a function of the lateral cover L_c.

Its application to simulate the Martian dust emissions requires input data concerning the surface features on Mars, in particular surface roughness data. The spatial variation of the surface roughness has not been fully investigated yet on Mars, and latest MGCM simulations have assumed a spatially uniform value within the 0.001-0.01m range [5, 6, 7] estimated for the Viking lander and Pathfinder sites [8, 9].

Data description: We have tested the possibility of using rock abundance maps derived from thermal inertia to estimate the surface roughness on Mars [10, 11, 12]. These rock abundance maps have been further validated using rock-size frequency distributions inferred from different martian landing sites and Earth analogs. Previous works on this topic have been mainly dedicated to better assess the quality of the landing sites [13, 14, 15, 16].

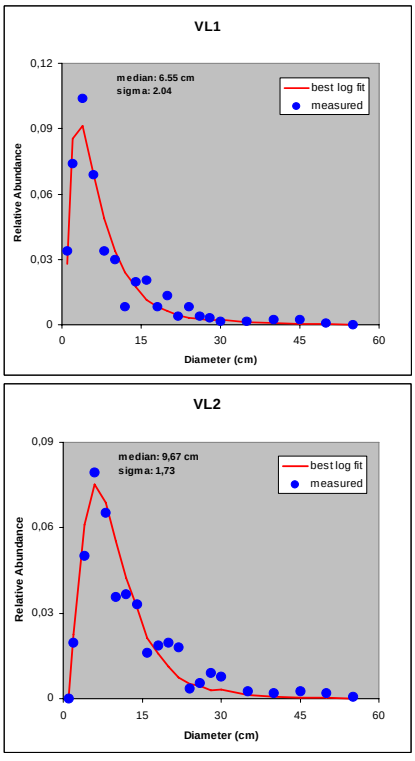

Fig. 2. Histograms reporting the number of rocks for each size bin diameter at Viking landers 1 and 2 sites and the fitted log-normal distributions.

As a consequence, the attention has been mainly focused on the bigger rocks distribution, a critical point for characterizing a landing site, that is well repro-

duced by their chosen exponential fits to the observational data. However, surface roughness can be principally driven by the smallest rocks, and log-normal distributions seem to be better adapted to reproduce with a comparable quality the various-sized components (Fig. 2). We will discuss the implications of our surface roughness calculations for different landing sites.

Results and discussion: Rock abundances have been converted to surface roughness to allow computation of the aeolian erosion thresholds (Fig. 3). A map of these aeolian erosion thresholds has been established and associated with climatological surface wind velocities to identify the Martian regions exhibiting the highest potential for dust emissions (Fig. 4).

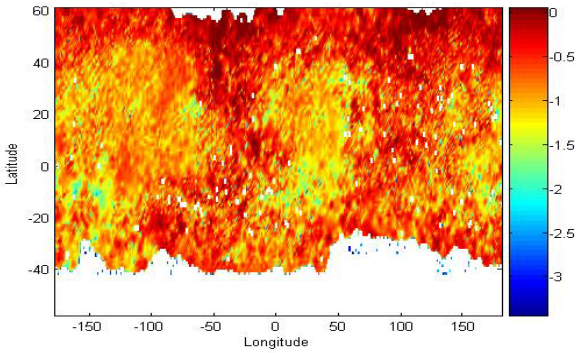

Fig. 3. Logarithm of the aerodynamic roughness height Z_0 (in cm).

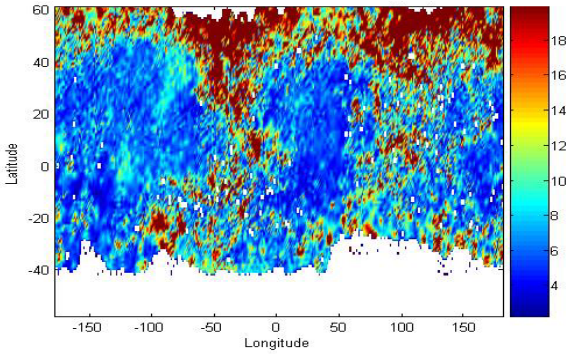

Fig. 4. Minimal threshold wind friction velocity ($m.s^{-1}$)

References: [1] Cantor (2007), *Icarus 186*, 60–96. [2] Basu et al. (2006), *JGR 111(E9)*, E09004. [3] Marticorena and Bergametti (1995), *JGR 100(D8)*, 16415-16430. [4] Marticorena et al. (1997), *JGR 102(D4)*, 4387-4404. [5] Newmann et al. (2002), JGR 107(E12), 5123. [6] Montabone et al. (2005), Adv. Space Res. 36, 2146–2155. [7] Kahre et al. (2006), JGR 111(E6), E06008. [8] Sutton et al. (1978), J. Atmos. Sci. 35, 2346–2355. [9] Sullivan et al. (2000), *JGR 105(E10)*, 24547-24562. [10] Christensen (1986), *Icarus 68*, 217-238. [11] Golombek et al. (2003), *JGR 108(E12)*, E128086. [12] Putzig (2006), *PhD thesis*. [13] Golombek and Rapp (1997), *JGR 102(E2)*, 4117-4129. [14] Golombek et al. (2003), *JGR 108(E12)*, E128086. [15] Golombek et al. (2005), *Nature 436*, 44-48. [16] Golombek et al. (2007), *LPS XXXVIII*, 1405.

Aknowledgment: This work was supported by the Centre National d'Etudes Spatiales (CNES) .